
Supporting Information

Au@TiO₂ Yolk-Shell Hollow Spheres for Plasmon-Induced Photocatalytic Reduction of CO₂ into Solar Fuel via Local Electromagnetic Field

Wenguang Tu,^{a, b, c} Yong Zhou,^{*, a, b, c} Haijin Li,^{b, c, e} Ping Li,^{b, c} and Zhigang Zou^{*, b, c, d}

^aKey Laboratory of Modern Acoustics, MOE, Institute of Acoustics, School of Physics, Nanjing University, Nanjing 210093, P. R. China; E-mail: zhouyong1999@nju.edu.cn

^bNational Laboratory of Solid State Microstructures, Department of Physics, and Collaborative Innovation Center of Advanced Microstructures Nanjing University, Nanjing 210093, China; E-mail: zgzou@nju.edu.cn

^cEcomaterials and Renewable Energy Research Center (ERERC), Nanjing University, Nanjing 210093, China

^dDepartment of Materials Science and Engineering, Nanjing University, Nanjing 210093, P. R. China

^eSchool of Mathematics and Physics, Institute of Optoelectronic Information Materials and Technology, Anhui University of Technology, Ma'anshan 243002, P. R. China

Experimental:

Materials: $\text{HAuCl}_4 \cdot 3\text{H}_2\text{O}$ (99.9+%) and Tetrabutoxide titanate (TBOT) were purchased from Alfa Aesar. Distilled water was used in all experiments.

Synthesis of Au-cored carbon spheres: Au-cored carbon spheres were prepared as previous report.^[1] A solution of HAuCl_4 (0.5 mL, 0.02 M) was added to a glucose solution (40 mL, 6g) with stirring to form a clear solution, which was transferred to a Teflon autoclave and treated at 180°C for 6 hr. Pure carbon spheres with the same diameter was prepared by treating Teflon autoclave with a glucose solution (40 mL, 6g) at 180°C for 12 hr.

Synthesis of Au@TiO₂ yolk-shell hollow spheres: Coating TiO₂ on the core templates was prepared via a versatile kinetics-controlled coating method.^[2] The core templates were dispersed in absolute ethanol (100 mL), and mixed with concentrated ammonia solution (0.30 mL, 28 wt%) under ultrasound for 15 min. Afterward, 0.5 mL of TBOT was added dropwise in 5 min, and the reaction was allowed to proceed for 4 h at 50°C under continuous mechanical stirring. The resultant products were separated and collected, followed by washing with deionized water and ethanol for 3 times, respectively. Au@TiO₂ yolk-shell hollow spheres were produced by drying obtained powders by lyophilization, and calcining at 500 °C under N₂ for 2 hr and then in air for 2 hr to remove the organic species and improve crystallinity. For comparison, pure TiO₂ hollow spheres were prepared with the some processes.

Characterization: The morphology of the samples was observed by the field emission scanning electron microscopy (FE-SEM) (FEI NOVA NanoSEM230, USA)

and transmission electron microscopy (TEM) (JEOL 3010, Japan). The crystallographic phase of the as-prepared products was determined by powder X-ray diffraction (XRD) (Rigaku Ultima III, Japan) using Cu-K α radiation ($\lambda=0.154178$ nm) with scan rate of 10^0 min $^{-1}$ at 40 kV and 40 mA. The specific surface area of the samples was measured by nitrogen sorption at 77K on surface area and porosity analyzer (Micromeritics TriStar, USA) and calculated by the BET method. The UV-visible (UV-vis) diffuse reflectance spectra were recorded with a UV-vis spectrophotometer (UV-2550, Shimadzu) at room temperature and transformed to the absorption spectra according to the Kubelka–Munk relationship.

Photoelectrochemical measurement: The photocatalysts were deposited on FTO electrode used as working electrodes by electrophoresis deposition method in the same condition. To attach photocatalysts onto ITO glass, working electrodes were heated at 500 °C for 1 h in air. Photoelectrochemical measurements were carried out in a three-electrode configuration system: a FTO working electrode, Hg/Hg $_2$ Cl $_2$ as the reference electrode, and a Pt foil as the counter electrode. Na $_2$ SO $_4$ (0.5 M) aqueous solution was used as the electrolyte. The photocurrent was observed for each switch-on/off event by using a 500 W xenon lamp. The area of the samples exposed to light was 0.28 cm 2 . An applied potential of working electrode against the counter electrode was set to 0.6V.

Photocatalytic Experiments: In the photocatalytic reduction of CO $_2$, 0.01g of sample was uniformly dispersed on the glass reactor with an area of 4.2 cm 2 . A 300W Xenon arc lamp was used as the light source of photocatalytic reaction. The volume

of reaction system was about 230 ml. The reaction setup was vacuum-treated several times, and then the high purity of CO₂ gas was followed into the reaction setup for reaching ambient pressure. 0.4 ml of deionized water was injected into the reaction system as reducer. The as-prepared photocatalysts were allowed to equilibrate in the CO₂/H₂O atmosphere for several hours to ensure that the adsorption of gas molecules was complete. During the irradiation, about 1 ml of gas was continually taken from the reaction cell at given time intervals for subsequent CH₄ or C₂H₆ concentration analysis by using a gas chromatograph (GC-2014, Shimadzu Corp., Japan).

FDTD simulations: The finite difference time-domain (FDTD) simulations were run using the commercially available Optiwave software to simulate the propagation of light waves in arbitrary geometries. The field source is a 200–800 plane wave.

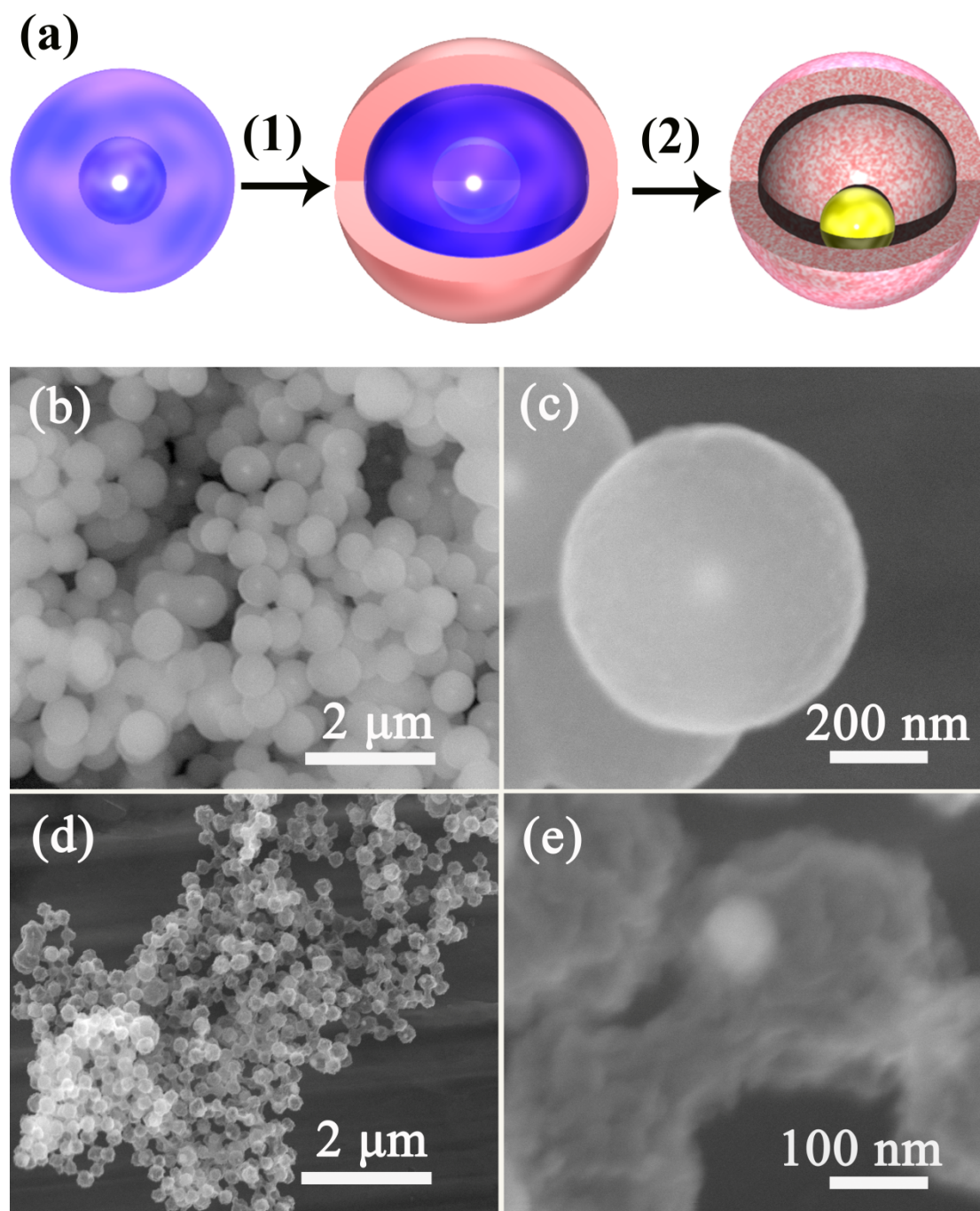


Fig. S1 (a) Illustration of the formation of Au@TiO₂ yolk-shell hollow spheres using Au-cored carbon spheres as templates: 1) amorphous TiO₂ coating (blue) on Au-cored carbon spheres; 2) annealing treatment to form Au@TiO₂ hollow spheres with highly crystalline and porous TiO₂ shells. (b, c) SEM images of Au@C@TiO₂ spheres, (d, e)

SEM images of Au@TiO₂ yolk-shell hollow spheres. Due to thin and smooth amorphous TiO₂ coating on Au-cored carbon sphere, the change of the shell surface is not obvious. After annealing treatment, the typical diameter of hollow spheres decreases and relatively rough surface appears, owing to the contraction effect caused by the decomposition of carbon spheres and the crystallization of TiO₂ shells.

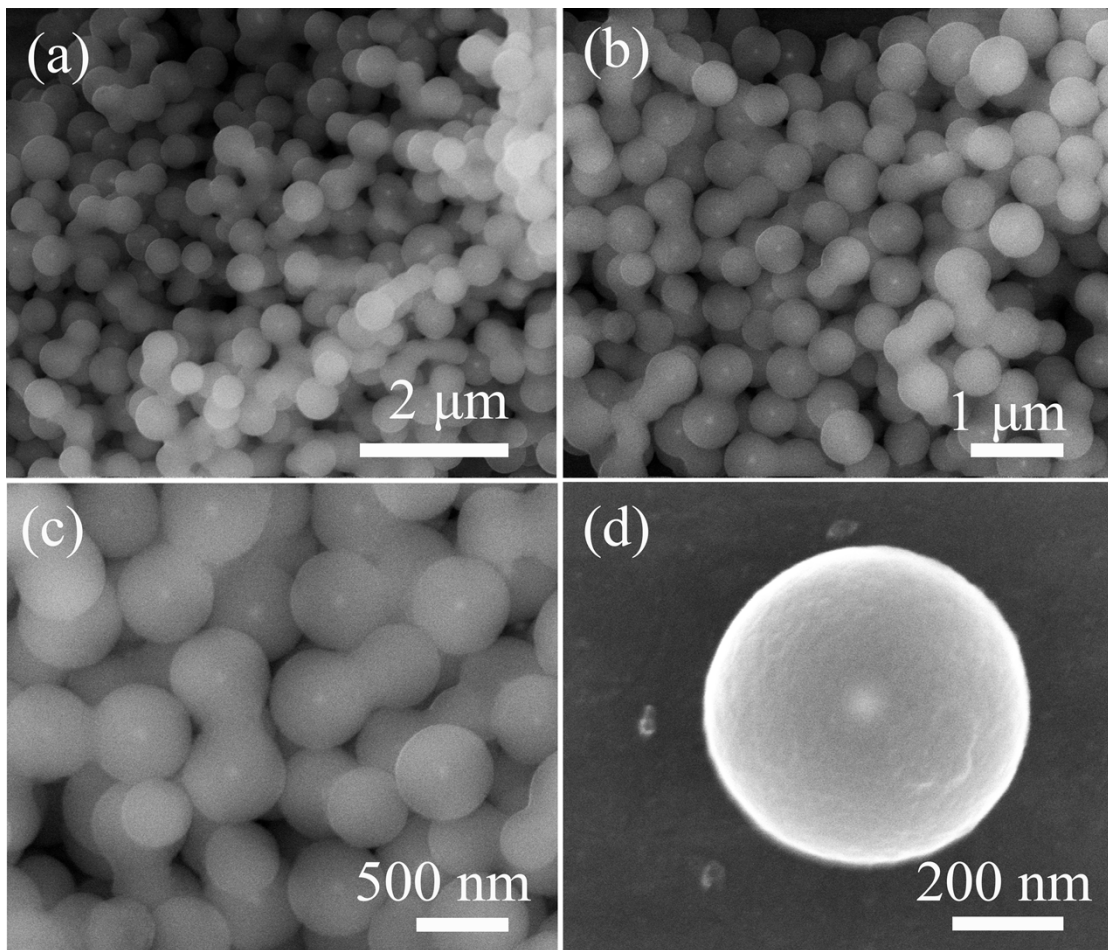


Fig. S2 (a-d) SEM images of Au-cored carbon spheres at different magnifications. In the hydrothermal process, glucose can act as a reducing agent to reduce Au ions into Au nanoparticles, and it undergoes carbonization to encapsulate Au nanoparticles into carbon spheres.

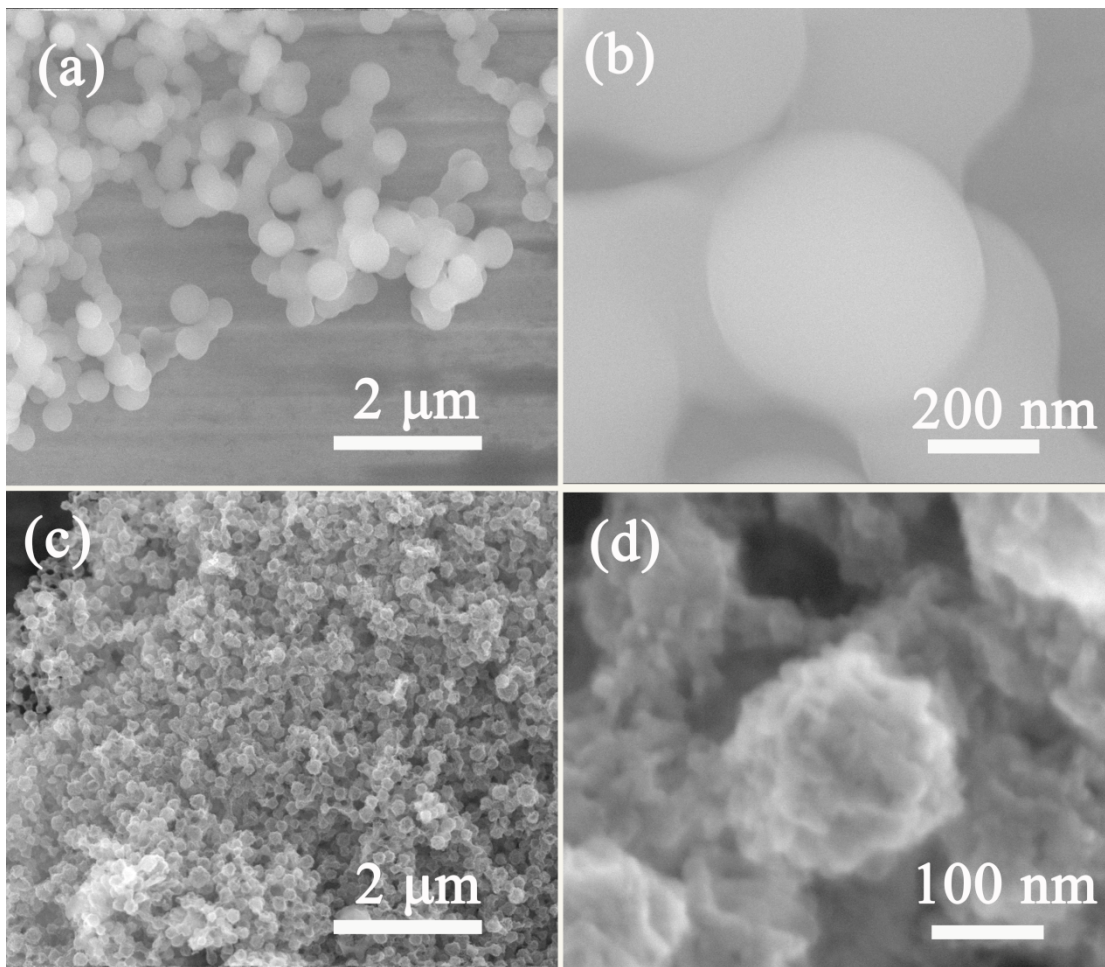


Fig. S3 (a, b) SEM images of pure carbon spheres, (c, d) SEM images of TiO₂ hollow spheres.

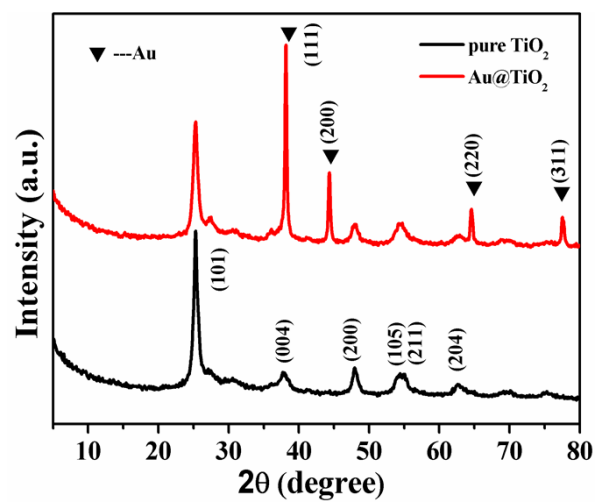


Fig. S4 XRD patterns of TiO_2 hollow spheres and Au@TiO_2 yolk-shell hollow spheres.

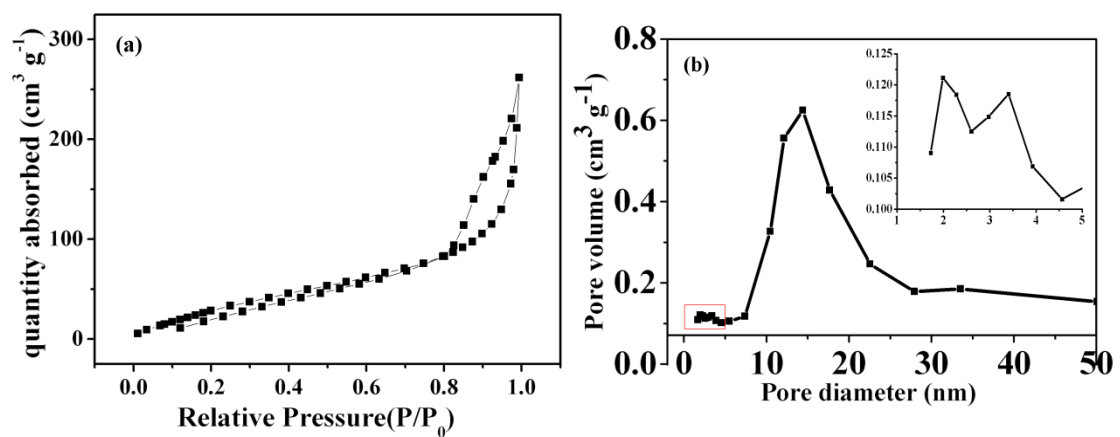


Fig. S5 Nitrogen adsorption–desorption isotherm (a) and the corresponding pore size distribution curves (b) of Au@TiO₂ yolk-shell hollow spheres. The inset in (b) is the part enlargement of the curve (red).

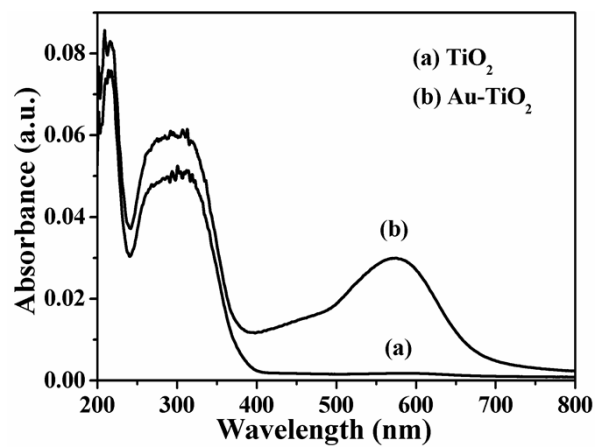


Fig. S6 UV-Vis diffuse reflectance spectra of TiO₂ hollow spheres (a) and Au@TiO₂ yolk-shell hollow spheres (b).

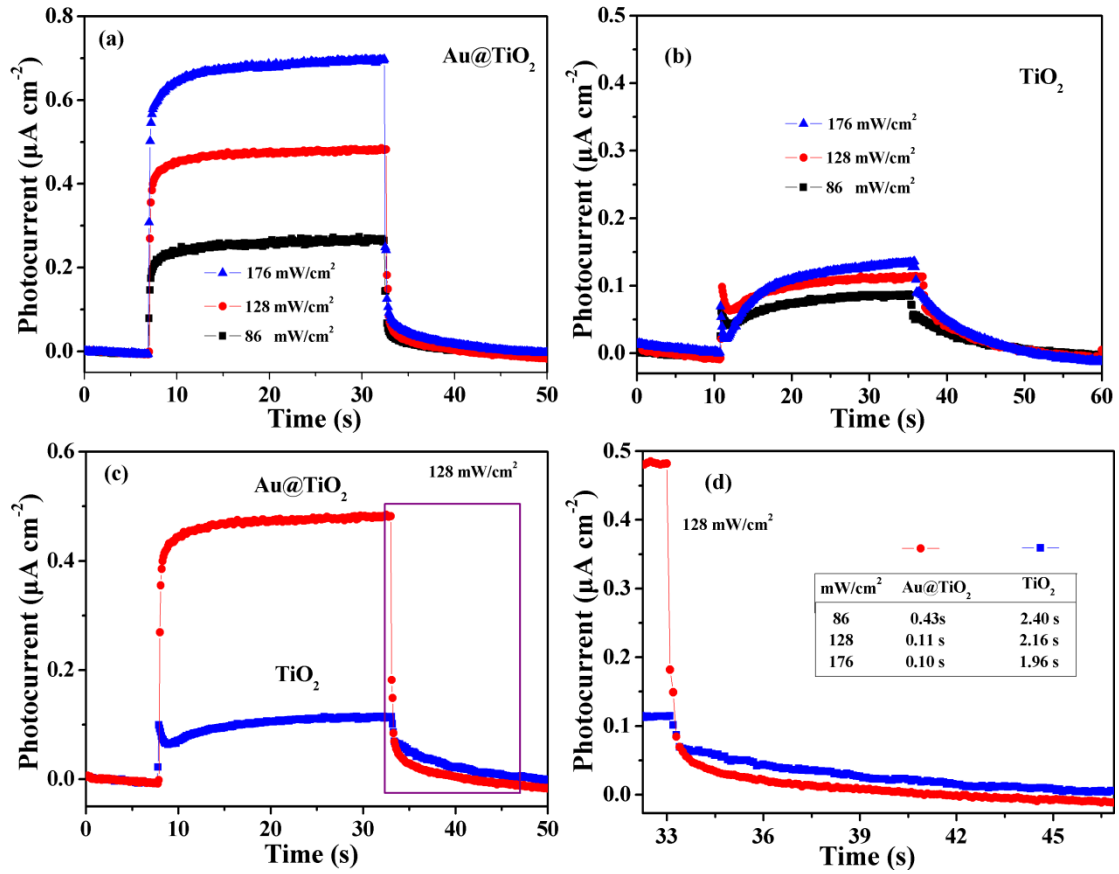


Fig. S7 Photocurrent responses of Au@TiO₂ yolk-shell hollow spheres (a) and (b) hollow spheres under light irradiation with different intensities. (c) The comparison of photocurrent of Au@TiO₂ yolk-shell hollow spheres TiO₂ and hollow spheres with light intensity of 128 mW/cm², and (d) is the enlargement of the inset box in the (c). The table in the (d) is the transient decay lifetime of surface trap states of Au@TiO₂ yolk-shell hollow spheres (a) and (b) hollow spheres under light irradiation with different intensities. The decay lifetime of each photocurrent time spectrum by fitting to a biexponential function function in the form of $f(t) = A_1 \exp(-t/\tau_1) + A_2 \exp(-t/\tau_2)$. The average lifetime τ is calculated by the expression in the form of $\tau = (A_1 \tau_1^2 + A_2 \tau_2^2) / (A_1 \tau_1 + A_2 \tau_2)$. This transient decay is an extrinsic surface state with long relaxation (~ 1 s), which is associated with adsorbed ions at the semiconductor

surface.^[3] The surface state may act in recombination of photogenerated electrons-hole pairs, whereas they also can perform a transit shipment of the photogenerated holes for the oxidation reaction.^[3]

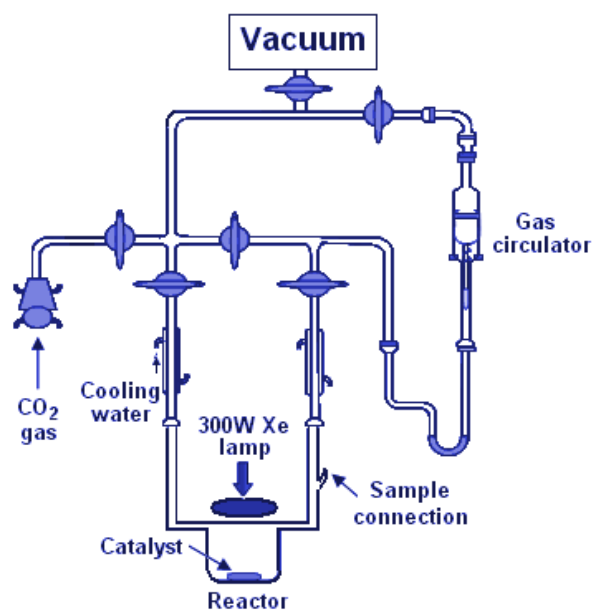


Fig. S8 Reaction setup for evaluation of conversion rate of CO₂.

References

- [1] X. M. Sun, Y. D. Li, *Angew. Chem. Int. Edit.* **2004**, *43*, 597-601.
- [2] W. Li, J. P. Yang, Z. X. Wu, J. X. Wang, B. Li, S. S. Feng, Y. H. Deng, F. Zhang, D. Y. Zhao, *J. Am. Chem. Soc.* **2012**, *134*, 11864-11867.
- [3] Z. S. Li, W. J. Luo, M. L. Zhang, J. Y. Feng, Z. G. Zou, *Energ. Environ. Sci.* **2013**, *6*, 347-370.